Mobile robot navigation in unknown environment based on exploration principles

Arvanitakis, I., Giannousakis, K. & Tzes, A.

DOI 10.1109/CCA.2016.7587878
ISBN 978-1-5090-0756-1

Publisher: IEEE

Mobile Robot Navigation in Unknown Environment based on Exploration Principles

Ioannis Arvanitakis, Konstantinos Giannousakis and Anthony Tzes

Abstract— **This article focuses on the mobile robot's autonomous navigation problem in an unknown environment. Considering a robot equipped with an omnidirectional range-sensor a map of the discovered area is constructed in an iterative manner. Given a target position located in the unexplored territory, initially a motion planning scheme is employed that relies on exploration-principles of the area near the target. This is achieved by assigning an exploration cost function that indirectly attracts the robot close to target. Upon discovery of the target, the robot moves to it following the shortest-distance path. Simulation studies that prove the efficiency of the overall method are presented.**

I. Introduction

Autonomous navigation of mobile robots is an area of research with increasing interest over the years due to recent technological advances [1]. Tasks such as area coverage [2–4] and exploration, surveillance, search and rescue missions require that the robots move efficiently in the environment, avoiding obstacles during motion and keeping under consideration the robots' physical constraints. Motion planning for known environments has been extensively researched over the past few decades [5]. Popular motion planning solutions for known environments include, but not limited to, the Artificial Potential Fields method [6], the vector field histogram [7], probabilistic roadmaps [8] and Rapidly-exploring Random Trees (RRT) [9].

In the latest years a paradigm shift towards motion planning in uncertain or unknown environments has been noted. In these scenarios, the robot is equipped with a sensor – in most cases a sonar, lidar, or stereo vision based system – that provides information about the environment, resulting in an online map building process. These sensors have either limited sensing range capabilities or the sensor readings may be considered unreliable after a specific limit. One of the first proposed methods, to account for this sensing-scenario, was the Dynamic Window Approach [10] combining concepts from real time obstacle avoidance and motion planning to calculate the admissible velocities that steer the robot towards the target. In [11] the authors propose a partially closed loop receding horizon control algorithm to navigate in dynamic and uncertain environments, while in [12] a gap sensor that tracks discontinuities in depth information for the creation of a gap navigation tree for efficient navigation is utilized.

In terms of entirely unknown environments, most methods focus mainly on local real time obstacle avoidance as they try to reach the unknown target area. These methods may be effective but tend to produce paths that lead the robot close to obstacles [13], leading in robot configurations that are inefficient both in terms of area sensing and avoiding potential new obstacles. Furthermore, from an exploration point of view, the target area is an unknown segment of the environment that the robot needs to discover. Motion planning in these situations may be closely connected with exploration process; the robot should utilise the existing information about the discovered environment and plan an optimal path towards the unknown target area. One of the first methods is the frontier based exploration, where a frontier is defined as the boundary between explored and unexplored space. The robot attempts to move towards the closest frontier to its position [14], referred to as the MinDist approach in the literature. The DisCoverage algorithm [15] utilizes the concept of frontier based approach by selecting appropriate target points along the frontiers for convex environments and then the authors extend it for non-convex environments [16] by transforming the non convex domain to a star shaped domain. The authors in [17], solve the coverage problem on non-Euclidean spaces through the generalization of Lloyd's algorithm, by proper selection of coverage functional, and present the application of this method for exploration. In most scenarios, a group of robots is deployed within the unknown area. The problem though may be degenerated into a single robot exploration problem by utilising a Voronoi tessellation algorithm for subspace exploration assignment [18] and then applying single robot exploration methods.

The novelty of the present work is the navigation of a mobile robot in an unknown environment towards a goal position based on frontier exploration principles. A robot equipped with a limited range omnidirectional sensor is located in an unknown environment, where only the goal location is known. To discover the goal location and plan a path towards it, the robot takes into account the explored area to find a frontier for exploration by minimizing a cost function. The proposed control law then aims to guide the robot towards the frontier strictly within the feasible explored space, via a gradient ascent method of an objective function. This process is executed until the target location is found, where then the robot creates a simple geodesic based navigation function to create the final path segment.

In Section II mathematical preliminaries and the problem formulation is given, followed by the authors' suggested algorithm in Section III. In Section IV simulation results that prove the efficiency of the proposed scheme are offered, while in Section V conclusions are outlined.

The authors are with the Department of Electrical & Computer Engineering, University of Patras, Rio 26500, Greece.
Corresponding author's e-mail: tzes@ece.upatras.gr

II. Problem Formulation

A. Mathematical Preliminaries

Consider a path-connected topological space $\mathcal{A} \subset \mathbb{R}^n$. The boundary of $\mathcal{A}$ is denoted as $\partial\mathcal{A}$, while $\{\mathcal{B}_i\}$, $i = 1, ..., N$ denotes a collection of subsets. Spaces $\mathcal{A}, \mathcal{B}$ are considered disjoint if $\mathcal{A} \cap \mathcal{B} = \varnothing$.

For connected spaces, the Euclidean metric $d(p_1, p_2) = \|p_1 - p_2\|$ is not an optimal norm for defining the distance between two points. Instead, the geodesic metric is introduced; that is given the collection of all paths $\{\gamma_k\}$ that connect two arbitrary points $p_1, p_2 \in \mathcal{A}$, the length of the shortest path defines the geodesic metric $d_g(p_1, p_2)$ and the resulting path is called the geodesic path. With the help of the geodesic metric, the geodesic Hausdorff distance is introduced which a special case of the Hausdorff metric [19].

Definition 1: Let us consider $p \in \mathcal{A}$ and a subspace $\mathcal{B} \subseteq \mathcal{A}$. Then the geodesic Hausdorff distance is defined as the minimum geodesic distance of all points $q \in \mathcal{B}$ from p, i.e.

$$H_g(p, \mathcal{B}) = \min_{q \in \mathcal{B}} d_g(p, q) \ .$$

Definition 2: Consider a point $p \in \mathcal{A}$. The visibility subspace of $\mathcal{A}$ from p is defined as a subset $\mathcal{A}^v(p; R)$, containing all points q, so that the geodesic path connecting p and q is a straight line and has length less than or equal to R, i.e.

$$\mathcal{A}^v(p; R) = \{q \in \mathcal{A}; d_g(p, q) = \|p - q\| \leq R\},$$

where $R \in \mathbb{R}_+ \cup \{\infty\}$.

In Fig. 1 an example for a path-connected (non-simply connected) space and its visibility subspace from an arbitrary position is depicted.

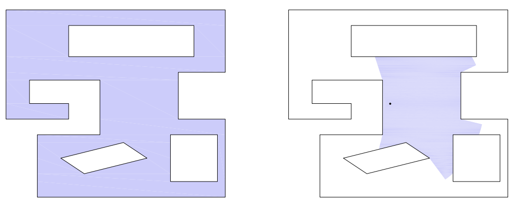

(a) (b)

Fig. 1: Path connected space (left) and visibility subspace from an arbitrary position (right)

Regarding notations, $\mathbb{I}_n$ and $\mathbb{O}_n$ denote the $n \times n$ identity and zero matrix respectively, while $L[\partial\mathcal{A}_k]$ denotes the length of the boundary segment $\partial\mathcal{A}_k$.

B. Problem Statement

Let $\Omega \subset \mathbb{R}^2$ be the unknown area of interest, which may be considered as a path connected space. Let $r \in \Omega$ be the position of a robot and $p_t \in \Omega$ be a goal position. The robot is equipped with an omnidirectional range sensor of circular pattern, with a sensing limit R. We assume perfect knowledge of the position of the robot and noiseless measurements from the sensor. At any time instance, a visibility subspace $\mathcal{S} = \Omega^v(r; R)$ created by the range sensor is defined, while $\mathcal{A} \subseteq \Omega$ is the aggregated sensed area; it is apparent that $\mathcal{S} \subseteq \mathcal{A}$.

The robot's kinodynamic model is

$$\dot{r} = u \ , \tag{1}$$

where $r \in \Omega$ and $u \in \mathbb{R}^2$.

Initially, the target belongs to the unknown area and is to be discovered. To account for this discovert, an objective function is formulated

$$\mathcal{H}(r) = \max \int_{\mathcal{S}} f(p)\phi(p)dp \ , \tag{2}$$

where, a) $f(p) : \mathcal{A} \to \mathbb{R}$ is a performance function that describes the performance in terms of exploration – gain of information – of different areas in $\mathcal{A}$, and b) $\phi(p) : \mathcal{A} \to \mathbb{R}$ is a weighting function that describes the importance of different areas in terms of a specific task assignment. In pure exploration missions,$\phi(p) = 1$. Since in this work, we are primarily interested in the navigation towards a target area in unknown space, then this function takes its maximum value at p_t, ot $\max_{\phi \in \Omega} = \phi(p_t)$.

It is apparent, that within the noted cost in (2) describe in a concurrent manner exploration (through $f(q)$) and navigation (through $\phi(q)$) aspects. If $p_t \in S$, and henceforth being 'visible' from the current location of the robot, then the cost function switches to

$$\mathcal{H}(r)|_{p_t \in S} = \max \frac{1}{\|p_t - r\|} \ , \tag{3}$$

and the robot uses the shortest path towards the 'visible' target point.

III. Path Planning

A. Control Law Derivation

The task goal initially is to find a control law that maximizes at each time step the objective function (2). Differentiating $\mathcal{H}(r)$ with respect to r yields,

$$\frac{\partial \mathcal{H}}{\partial r} = \frac{\partial}{\partial r} \int_{\mathcal{S}} f(p)\phi(p)dp \ ,$$

and by utilizing the Leibniz integral rule we obtain,

$$\frac{\partial \mathcal{H}}{\partial r} = \int_{\partial \mathcal{S}} f(p)\phi(p)\frac{\partial p}{\partial r} n dp \ , \tag{4}$$

where n is the outward unit normal vector to $\partial\mathcal{S}$.

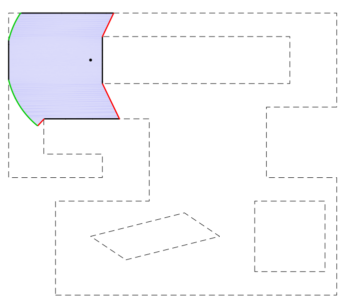

Fig. 2: $\partial\mathcal{S}$-boundary decomposition

The boundary $\partial\mathcal{S}$ can be decomposed into: a) a collection of l-segments that belong to visible area boundaries $\{\partial\mathcal{S}_l^o\} \subseteq \partial\Omega$, b) a collection of k-circular arcs $\{\partial\mathcal{S}_k^c\}$ created by the limit range of the sensor, and c) a collection of l-line segments $\{\partial\mathcal{S}_m^\ell\}$ created by visibility constraints that may be denoted as $\{[a,b]_k\}, \|a-r\| < \|b-r\|$. A visualization depicting the above is illustrated in Fig. 2, where the visible boundary edges $\{\partial\mathcal{S}_l^o\} \subseteq \partial\Omega$ (solid black lines), the circular arcs $\{\partial\mathcal{S}_k^c\}$ (green curves) and the line segments $\{[a,b]_k\}$ (red lines) are distinguished. It should be noted that segments $\{[a,b]_k\}$ have no immediate physical interpretation as there is no direct visibility, thus it can be either a free boundary or be part of $\partial\Omega$. The utilized control law though should take these segments into consideration, and treats them as free boundaries. Consequently, $\partial\mathcal{S}$ may be written as,

$$\partial\mathcal{S} = \bigcup_{i=1}^{l} \partial\mathcal{S}_i^o + \bigcup_{i=1}^{k} \partial\mathcal{S}_i^c + \bigcup_{i=1}^{m} \partial\mathcal{S}_i^\ell \ . \tag{5}$$

Equation (4) is thus transformed to

$$\begin{aligned} \frac{\partial\mathcal{H}}{\partial r} &= \sum_{i=1}^{l} \int_{\partial\mathcal{S}_i^o} f(p)\phi(p)\frac{\partial p}{\partial r} n dp \ + \\ & \sum_{i=1}^{k} \int_{\partial\mathcal{S}_i^c} f(p)\phi(p)\frac{\partial p}{\partial r} n dp + \sum_{i=1}^{m} \int_{\partial\mathcal{S}_i^\ell} f(p)\phi(p)\frac{\partial p}{\partial r} n dp \ . \end{aligned} \tag{6}$$

Each term of (6) implicates the need to compute $\partial p/\partial r$. The first term is zero, since $\partial p/\partial r|_{r\in\partial\Omega} = \mathbb{O}_2$. For the second term, $\partial p/\partial r|_{r\in\partial\mathcal{S}_i^c} = \mathbb{I}_2$, since all point on the boundary of the circular arcs move with the same velocity as the robot. For the last term, p can be expressed as

$$p = a_\ell + \upsilon_\ell(b_\ell - a_\ell) \ , \upsilon_\ell \in [0,1] \, . \tag{7}$$

Differentiating (7) leads to

$$\frac{\partial p}{\partial r} = \upsilon_\ell \frac{\partial b_\ell}{\partial r} \ , \upsilon_\ell \in [0,1] \ . \tag{8}$$

Considering $\partial b_\ell/\partial r$, further elaboration is required. Infinitesimal movement of point r will give point b_ℓ a velocity ν_b that can be analysed into an angular component ν_b^a created by a possible rotation of r around point a_ℓ and a translational component ν_b^t along the direction of vector $\overrightarrow{a_\ell b_\ell}$. The translational component ν_b^t is neglected as the boundary is mainly affected from the rotational movement around a_ℓ. Regarding component ν_b^a it is proven that

$$\nu_b^a \ = \ \omega \times (p_b - p_a) = -\frac{\|p_b - p_a\|}{\|r - p_a\|}\nu_r^a \ .$$

From the above it can be deducted that

$$\frac{\partial p}{\partial r}|_{r\in S^\ell} = -\frac{\|p_b - p_a\|}{\|r - p_a\|}\upsilon \mathbb{I}_2 \ . \tag{9}$$

Taking the previous analysis into consideration, equation (6) takes the form,

$$\begin{aligned} \frac{\partial\mathcal{H}}{\partial r} &= \sum_{i=1}^{k} \int_{\partial\mathcal{S}_i^c} f(p)\phi(p) n dp \ + \\ & \sum_{i=1}^{m} \int_0^1 f'(\upsilon)\phi'(\upsilon)\left(-\frac{\|p_b - p_a\|}{\|r - p_a\|}\right)\|b_i - a_i\|\upsilon n d\upsilon \ . \end{aligned} \tag{10}$$

where $f'(\upsilon) = f(a_i + \upsilon(b_i - a_i))$ and $\phi'(\upsilon) = \phi(a_i + \upsilon(b_i - a_i))$ respectively.

Using $u = \frac{\partial\mathcal{H}}{\partial r}$ from (10) as the control input of the robot results to the maximization of (2), since

$$\frac{d\mathcal{H}}{dt} = \frac{\partial\mathcal{H}}{\partial r}\frac{dr}{dt} = \left\|\frac{\partial\mathcal{H}}{\partial r}\right\|^2 \geq 0 \ . \tag{11}$$

As mentioned in subsection II-B, this control input is applied to the robot until the target area is discovered, at which point the control law switches to a navigation function based on the shortest distance to target, $d_g(r, p_t)$ and the gradient descent law constructs the final segment of the path.

B. Exploration Frontier Selection

In the previous subsection it was proven that $u = \frac{\partial\mathcal{H}}{\partial r}$ maximizes over time the objective function (2), a navigation optimality criterion that relates to the selection of $f(p)$ and $\phi(p)$, while the overall scheme is based on a frontier based exploration process.

In a manner similar to the collection decomposition of boundary $\partial\mathcal{S}$, boundary $\partial\mathcal{A}$ is decomposed into two collections, $\{\partial\mathcal{A}_l^o\} \subseteq \Omega$ and free boundaries $\{\partial\mathcal{A}_k^f\}$. It should be noted that from the moment that $\mathcal{A}$ is the aggregated union over time of $\mathcal{S}$, a single frontier $\partial\mathcal{S}_k^f$ may either be a curve created by the sensing limit, a line created by the visibility constraint or a combination of both. The line segments as mentioned in the previous subsection, have no immediate physical interpretation, should be treated ideally as a different kind of frontier as in $\partial\mathcal{S}$ as in the case of equation (5); in this case however there is an inherent complexity of this distinction so curve segments and line segments for simplicity are considered to belong to the same collection.

Frontier selection should take into account the proximity of the frontier to the target, the proximity of the robot to the frontier and the accessibility to new unexplored areas. To implicate the proximity to target the introduction of space $\overline{\mathcal{A}} = \left(\mathbb{R}^2 \setminus \mathcal{A}\right) \cup \partial\mathcal{A}$ is required initially which unlike $\mathcal{A}$ is not connected, but comprises from a collection of simply connected disjoint subsets. The frontier search is then limited to those frontiers that are boundaries of the disjoint subset $\overline{\mathcal{A}}_d \subset \overline{\mathcal{A}}$ that contains the target. The geodesic Hausdorff distance of a frontier from the target is then eligible to be used $H_g(p_t, \partial\mathcal{A}_k^f)$. This distance given the existing information about the explored area relates with the distance the robot will need to traverse in the unknown area to reach the target. Furthermore in space $\mathcal{A}$ the geodesic Hausdorff distance of the robot from a frontier $H_g(r, \partial\mathcal{A}_k^f)$ is calculated, which estimates the cost of moving towards a frontier. Frontiers with relatively small values of $H_g(p_t, \partial\mathcal{A}_k^f)$ and $H_g(r, \partial\mathcal{A}_k^f)$ can initially be selected, but their length may be relatively small compared to other frontiers, which make them unsuitable for exploration as they potentially offer less accessibility to unexplored areas compared to frontiers with larger lengths. This is taken into account into the cost function responsible for the frontier selection, which takes the following form:

$$\begin{aligned}\partial\mathcal{A}_c^f &= \arg\min_j \Big(w_1 L\left[\partial\mathcal{A}_j^f\right]^{-1} + \\ &\qquad w_2 H_g(p_t, \partial\mathcal{A}_j^f) + w_3 H_g(r, \partial\mathcal{A}_j^f) \Big) \ , \quad (12)\end{aligned}$$

where $w_i \in [0,1], i = 1,2,3$ are weights assigned to each part of the cost function. Equation (12) is evaluated constantly in conjunction with the control law, as more suitable frontiers might emerge from the ongoing exploration such in the case when a frontier reduces in length significantly or breaks into two or more new frontiers – referred as the 'crossroad situation'.

C. Performance and weighting functions selection

As mentioned in subsection II-B, the performance function $f(p)$ implicates the exploration process into the objective given by (2) and weighting function $\phi(p)$ implicates the navigation towards the desired position. The performance function will be defined as:

$$f(p) = \frac{1}{H_g(p, \mathcal{A}_c^f) + 1} \quad (13)$$

The aforementioned performance function ensures that areas near the exploration frontier will be of greater importance than areas further away from it. In an intuitive manner, the robot will move towards the closest neighbourhoods of the frontier, which would potentially lead it away from the target area. To avoid this the weighting function $\phi(p)$ is defined as

$$\phi(p) = \frac{1}{d_g(y, p_t) + 1} \ , \quad (14)$$

$$y = \arg\min_{y \in \mathcal{A}_c^f} H_g(p, \mathcal{A}_c^f) \ . \quad (15)$$

It must be noted that $d_g(y, p_t)$ refers to space $\overline{\mathcal{A}}$. This selection gives greater importance in neighbourhoods of $\mathcal{A}_c^f$ that are closer to the target than neighbourhoods further away from it.

IV. Simulation studies

The efficiency of the proposed scheme is verified through two different simulation scenarios. Two different areas for navigation were created that are depicted in Fig. 3, where for visualization purposes the target position (black dot) is also illustrated.

In the first scenario (Fig. 3(a)) the rectangle encapsulating the convex hull of Ω is of $14m \times 12m$. The robot has a range sensor of $R = 1.3m$ and at each iteration step the robot moves along the direction given by equation (10) with a constant velocity of $\nu = 0.1m$, while the weights of equation (12) are selected as $w_1 = 1, w_2 = 0.9$ and $w_3 = 0.4$. The boundary at each step of the explored area is archived using an OctoMap [20] like method with a grid resolution of $0.05m$.

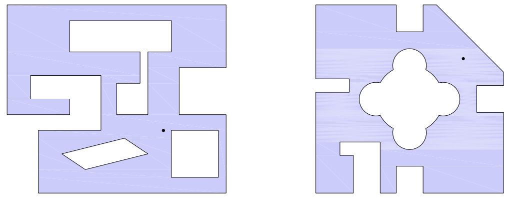

(a) (b)

Fig. 3: Ω-sample areas for navigation

In Fig. 4, the evolution of the navigation towards the target area is seen, where the grey area depicts the unknown space and the explored space corresponds to 'light blue'. Discovered area boundaries are depicted with black, while with red the frontiers are depicted, and blue depicts the selected frontier given from equation (12). As may be seen in Figs. 4(b) and (c), equation (12) is able to select the optimal frontier to explore and is capable of switching efficiently to new frontiers whenever the existing frontier gives a suboptimal cost function (Fig. 4(d)). In Fig. 4(e) the switching to the shortest path towards target takes effect as the target is within the explored space. As seen in Fig. 4(f) the resulting path is sufficiently far from the discovered area boundaries to account for safe and fast navigation, without danger of collision with obstacles.

In the second scenario (Fig. 3(b)) the area under investigation is of $14m \times 14m$. The robot has a range sensor of $R = 2m$ while the velocity is the same as the one in the first scenario. In this case the weights of equation (12) are selected as $w_1 = 0.8, w_2 = 0.6$ and $w_3 = 0.4$, while the grid resolution is kept the same at $0.05m$.

Similarly, in Fig. 5 the evolution of the navigation towards the target area is seen. In this scenario the effect of the exploration function into the control law given by equation (10) is better understood. Instead of simply avoiding obstacles, the robot selects a path to lead it towards the selected frontier in configurations away from the boundaries of the area as seen in Figs 5 (b) and (c). Giving greater importance to frontier length in equation (12) results in the frontier selection depicted in Fig. 5(d), which might create a lengthwise larger path and potentially guide it initially further away from target. Despite this, as seen in Fig. 5(f), the robot manages to effectively discover the target and guide towards it.

V. Conclusions

In this paper a novel method for navigation in unknown environments by a mobile robot is presented. The robot is equipped with a ranged omnidirectional sensor with limited sensing range and having accurate knowledge of its position. Taking into account a target location in the unknown area and the area that it has discovered so far, it selects via minimization of a cost function a suitable frontier for explo-

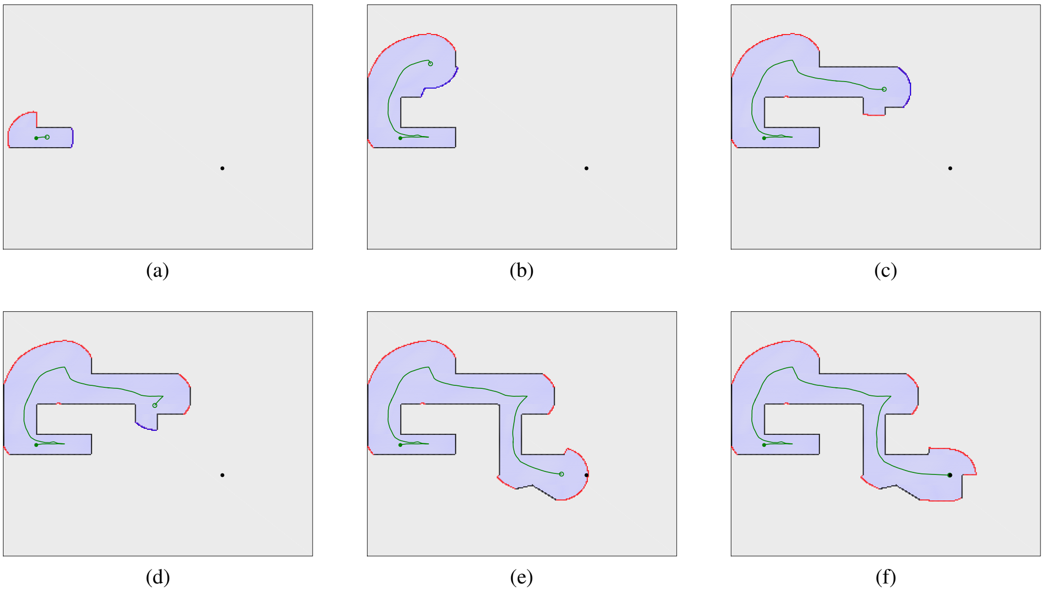
(a) (b) (c) (d) (e) (f)

Fig. 4: Evolution of the robot navigation towards the target location [1st scenario]

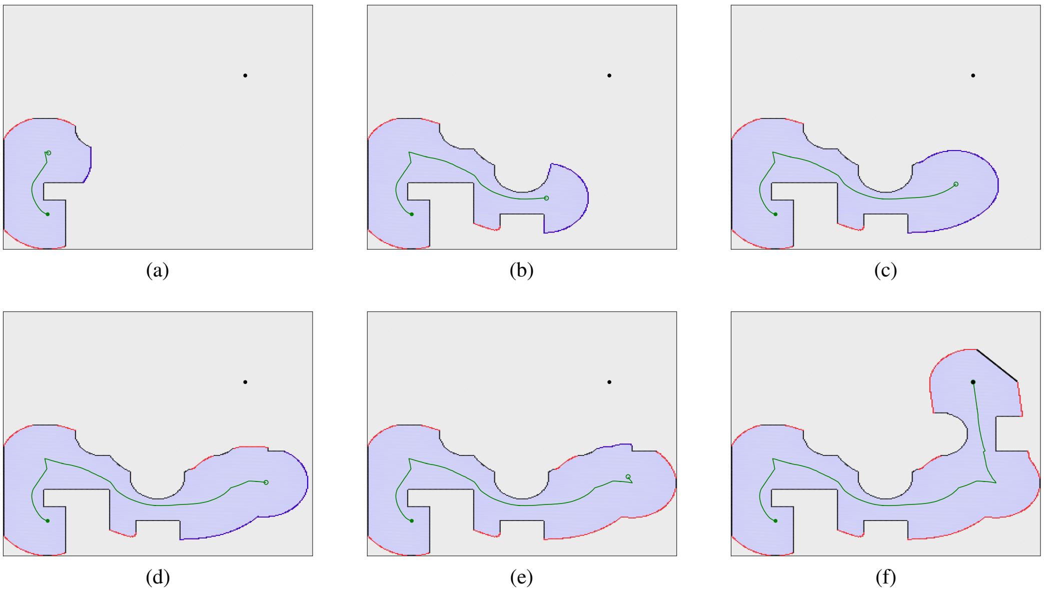
(a) (b) (c) (d) (e) (f)

Fig. 5: Evolution of the robot navigation towards the target location [2nd scenario]

ration. A control law is implemented that moves the robot along the direction that maximizes an objective function that implicates the exploration towards the unknown area near the target. As soon as the target area is found, the motion control law switches over to the shortest length navigation function. Simulation results that prove the efficiency of the proposed scheme are presented.

Acknowledgments

This work has received funding from the European Union Horizon 2020 Research and Innovation Programme under the Grant Agreement No. 644128, AEROWORKS.

References

[1] E. Garcia, M. Jimenez, P. De Santos, and M. Armada, "The evolution of robotics research," *Robotics Automation Magazine, IEEE*, vol. 14, no. 1, pp. 90 –103, March 2007.

[2] Y. Stergiopoulos, M. Thanou, and A. Tzes, "Distributed collaborative coverage-control schemes for non-convex domains," *IEEE Transactions on Automatic Control*, vol. 60, no. 9, pp. 2422–2427, 2015.

[3] Y. Kantaros, M. Thanou, and A. Tzes, "Distributed coverage control for concave areas by a heterogeneous robot-swarm with visibility sensing constraints," *Automatica*, vol. 53, pp. 195–207, 2015.

[4] Y. Stergiopoulos and A. Tzes, "Spatially distributed area coverage optimisation in mobile robotic networks with arbitrary convex anisotropic patterns," *Automatica*, vol. 49, no. 1, pp. 232–237, 2013.

[5] S. M. LaValle, *Planning Algorithms*. Cambridge, U.K.: Cambridge University Press, 2006.

[6] O. Khatib, "Real-time obstacle avoidance for manipulators and mo-

bile robots," in *Robotics and Automation. Proceedings. 1985 IEEE International Conference on*, vol. 2, Mar 1985, pp. 500 – 505.

[7] J. Borenstein and Y. Koren, "The vector field histogram-fast obstacle avoidance for mobile robots," *Robotics and Automation, IEEE Transactions on*, vol. 7, no. 3, pp. 278 –288, June 1991.

[8] L. Kavraki, P. Svestka, J.-C. Latombe, and M. Overmars, "Probabilistic roadmaps for path planning in high-dimensional configuration spaces," *Robotics and Automation, IEEE Transactions on*, vol. 12, no. 4, pp. 566 –580, Aug 1996.

[9] J. Kuffner, J.J. and S. LaValle, "RRT-connect: An efficient approach to single-query path planning," in *Robotics and Automation, 2000. Proceedings. ICRA '00. IEEE International Conference on*, vol. 2, 2000, pp. 995 –1001 vol.2.

[10] O. Brock and O. Khatib, "High-speed navigation using the global dynamic window approach," in *Robotics and Automation, 1999. Proceedings. 1999 IEEE International Conference on*, vol. 1, 1999, pp. 341–346 vol.1.

[11] N. Du Toit and J. Burdick, "Robot motion planning in dynamic, uncertain environments," *Robotics, IEEE Transactions on*, vol. 28, no. 1, pp. 101–115, Feb 2012.

[12] B. Tovar, R. Murrieta-Cid, and S. LaValle, "Distance-optimal navigation in an unknown environment without sensing distances," *Robotics, IEEE Transactions on*, vol. 23, no. 3, pp. 506–518, June 2007.

[13] A. Valero-Gomez, J. V. Gomez, S. Garrido, and L. Moreno, "The path to efficiency: Fast marching method for safer, more efficient mobile robot trajectories," *IEEE Robotics Automation Magazine*, vol. 20, no. 4, pp. 111–120, Dec 2013.

[14] B. Yamauchi, "A frontier-based approach for autonomous exploration," in *Computational Intelligence in Robotics and Automation, 1997. CIRA'97., Proceedings., 1997 IEEE International Symposium on*, Jul 1997, pp. 146–151.

[15] A. Haumann, K. Listmann, and V. Willert, "Discoverage: A new paradigm for multi-robot exploration," in *Robotics and Automation (ICRA), 2010 IEEE International Conference on*, May 2010, pp. 929–934.

[16] D. Haumann, A. Breitenmoser, V. Willert, K. Listmann, and R. Siegwart, "Discoverage for non-convex environments with arbitrary obstacles," in *Robotics and Automation (ICRA), 2011 IEEE International Conference on*, May 2011, pp. 4486–4491.

[17] S. Bhattacharya, R. Ghrist, and V. Kumar, "Multi-robot coverage and exploration on riemannian manifolds with boundaries," *The International Journal of Robotics Research*, vol. 33, no. 1, pp. 113–137, 2014.

[18] C. S. K. M. Wurm and W. Burgard, "Coordinated multi-robot exploration using a segmentation of the environment," in *Intelligent Robots and Systems, 2008. IROS 2008. IEEE/RSJ International Conference on*, Sept 2008, pp. 1160–1165.

[19] R. T. Rockafellar and R. J.-B. Wets, *Variational Analysis*. New York, USA: Springer, 1998.

[20] A. Hornung, K. M. Wurm, M. Bennewitz, C. Stachniss, and W. Burgard, "Octomap: an efficient probabilistic 3d mapping framework based on octrees," *Autonomous Robots*, vol. 34, no. 3, pp. 189–206, 2013.